BMC Biology

RESEARCH ARTICLE

Open Access

Sensing and avoiding sick conspecifics requires Gαi2$^+$ vomeronasal neurons

Jan Weiss[1*], Hélène Vacher[2†], Anne-Charlotte Trouillet[2†], Trese Leinders-Zufall[1], Frank Zufall[1*] and Pablo Chamero[2*]

Abstract

Background Rodents utilize chemical cues to recognize and avoid other conspecifics infected with pathogens. Infection with pathogens and acute inflammation alter the repertoire and signature of olfactory stimuli emitted by a sick individual. These cues are recognized by healthy conspecifics via the vomeronasal or accessory olfactory system, triggering an innate form of avoidance behavior. However, the molecular identity of the sensory neurons and the higher neural circuits involved in the detection of sick conspecifics remain poorly understood.

Results We employed mice that are in an acute state of inflammation induced by systemic administration of lipopolysaccharide (LPS). Through conditional knockout of the G-protein Gαi2 and deletion of other key sensory transduction molecules (Trpc2 and a cluster of 16 vomeronasal type 1 receptors), in combination with behavioral testing, subcellular Ca^{2+} imaging, and pS6 and c-Fos neuronal activity mapping in freely behaving mice, we show that the Gαi2$^+$ vomeronasal subsystem is required for the detection and avoidance of LPS-treated mice. The active components underlying this avoidance are contained in urine whereas feces extract and two selected bile acids, although detected in a Gαi2-dependent manner, failed to evoke avoidance behavior. Our analyses of dendritic Ca^{2+} responses in vomeronasal sensory neurons provide insight into the discrimination capabilities of these neurons for urine fractions from LPS-treated mice, and how this discrimination depends on Gαi2. We observed Gαi2-dependent stimulation of multiple brain areas including medial amygdala, ventromedial hypothalamus, and periaqueductal grey. We also identified the lateral habenula, a brain region implicated in negative reward prediction in aversive learning, as a previously unknown target involved in these tasks.

Conclusions Our physiological and behavioral analyses indicate that the sensing and avoidance of LPS-treated sick conspecifics depend on the Gαi2 vomeronasal subsystem. Our observations point to a central role of brain circuits downstream of the olfactory periphery and in the lateral habenula in the detection and avoidance of sick conspecifics, providing new insights into the neural substrates and circuit logic of the sensing of inflammation in mice.

Keywords LPS, Inflammation, Olfactory, Vomeronasal organ, Gαi2, V1R, Ca^{2+} imaging, Dendritic knob, Avoidance behavior, Lateral habenula

†Hélène Vacher and Anne-Charlotte Trouillet contributed equally to this work.

*Correspondence:
Jan Weiss
jan.weiss@uks.eu
Frank Zufall
frank.zufall@uks.eu
Pablo Chamero
pablo.chamero-benito@inrae.fr
Full list of author information is available at the end of the article

Background

Social behaviors facilitate interactions between conspecifics and increase the likelihood of the transmission of pathogens. Animals have developed behavioral mechanisms to minimize their exposure to infected individuals and to avoid contagion [1, 2]. In particular, rodents distinguish between infected and uninfected conspecifics on the basis of olfactory information, displaying avoidance of infected individuals [1, 3].

Olfactory-mediated social recognition depends largely on the accessory olfactory or vomeronasal system, including the detection of threats such as predator- or pathogen-derived molecules [4–8]. These chemical signals are detected by sensory neurons of the vomeronasal organ (VNO) through members of the vomeronasal type 1 receptor (V1R), vomeronasal type 2 receptor (V2R), and formyl peptide receptor (FPR) families [9, 10]. V1Rs and most FPRs are expressed in the apical VNO layer and use the G protein Gαi2 for signal transduction [11–14], whereas V2Rs and FPR3 employ Gαo signaling in the basal VNO [8, 15]. However, the molecular identity of the sensory neurons in the VNO responsible for the detection of sick conspecifics has remained elusive.

V1Rs are activated by small organic ligands present in urine and feces [14, 16–20], whereas V2Rs are activated by peptides present in urine, fur, or saliva [7, 15, 21, 22]. FPRs were originally identified as innate immune receptors activated by viral and bacterial metabolites and have been implicated in pathogen detection by the VNO [8, 13, 23, 24]. Mice often examine urine and feces and use olfactory cues derived from these sources to distinguish between infected and uninfected individuals. Such odor-driven activity ultimately must be represented and integrated by higher structures in the central nervous system (CNS) to cause active avoidance of infected individuals. Neither the source and chemical nature of the ligands that trigger the detection of sick conspecifics nor the neural circuits mediating avoidance responses have been well described.

We previously investigated chemosensory mechanisms underlying the detection of danger-associated metabolites and the execution of appropriate defense programs, including the sensing of predator cues, life-threatening environmental cues, and bacteria-derived metabolites [8, 25–27]. One important result from these studies was the finding that danger-associated olfactory stimuli causing defensive behaviors such as avoidance can be detected by multiple olfactory subsystems and involve a wide variety of cellular and molecular mechanisms.

Given these results, we here sought to investigate mechanisms underlying the sensing and avoidance of sick conspecifics using mice as experimental model. The first objective of this study was to employ mice that are in an acute state of inflammation induced by systemic administration of lipopolysaccharide (LPS, a component of cell walls of gram-negative bacteria) as a general indicator for the presence of pathogens [3] to gain new insight into the mechanisms mediating the sensing and avoidance of LPS-treated conspecifics. A second goal of this work was to obtain new information on the function of the Gαi2-expressing ($G\alpha i2^+$) subsystem of the VNO. Previous work has shown that this subsystem is involved in the balancing of territorial and infant-directed aggression [14], in the initial outcome of an acute competition [28], and in experience-dependent, VNO-mediated social behaviors [29]. Here, through conditional disruption of $G\alpha i2^+$ and other genes encoding key sensory transduction proteins—in combination with behavioral testing, cellular Ca^{2+} imaging, and pS6 and c-Fos neuronal activity mapping in freely behaving mice—we show that the $G\alpha i2^+$ vomeronasal subsystem also plays a central role in the detection and avoidance of sick conspecifics, and we identify the lateral habenula as a previously unknown CNS target involved in these tasks.

Results

Innate avoidance of LPS-treated mice requires Trpc2 and Gαi2 but is independent of the V1rab receptor cluster

Innate avoidance behavior can protect the host from infections and may reduce the spread of pathogens. Mice avoid conspecifics that are in an acute inflammatory state induced by injection of LPS [3], which mimics bacterial infection [30]. The VNO mediates this conspecific avoidance by detecting urinary cues from LPS-injected mice (LPS-urine) [3], but the molecular identity of the vomeronasal sensory neurons (VSNs) sensing these cues has not been characterized further. To identify VSN subpopulations that mediate the avoidance of sick conspecifics, we investigated the behavior of mice harboring three specific deletions of genes that are required for VNO signal transduction (Fig. 1).

First, we focused on the Trpc2 cation channel, the primary sensory ion channel in the VNO [5, 6, 31, 32]. We exposed healthy mice to anesthetized stimulus mice that were injected with either LPS or PBS control solution (Fig. 1a). The LPS-treated mice showed clear signs of sickness with reduced overall activity and an average drop in body temperature of 4.4 °C (LPS-treated: 33.8 ± 0.45 °C, $n = 17$; PBS-treated: 38.1 ± 0.19 °C, $n = 15$; Mann–Whitney ***, $p < 0.001$). We quantified the time that the test mouse investigated a stimulus animal during a 10-min exposure. Control C57BL/6N male mice (referred to as B6) spent more time investigating PBS-injected mice vs. LPS-injected mice (PBS: 46.2 ± 4.4 s, LPS: 30.4 ± 5.1 s, $p < 0.05$) (Fig. 1b). The investigation ratio revealed a clear preference for the healthy mouse ($\log_2$ investigation

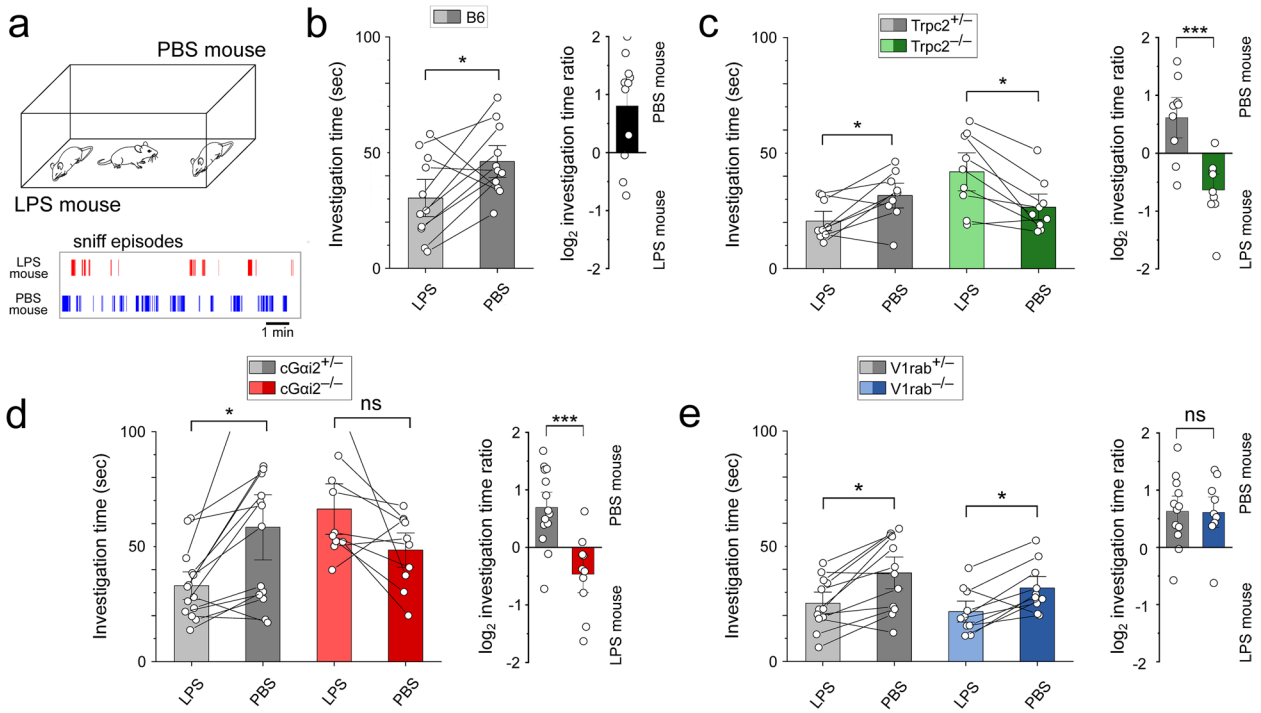

Fig. 1 Innate avoidance of LPS-treated mice requires Trpc2 and Gαi2 but is independent of the V1rab receptor cluster. **a** Male mice were allowed to investigate two anesthetized male conspecifics injected with either PBS or LPS. Bottom: representative scoring of the sniff episodes. **b**–**e** Investigation times and $\log_2$ investigation time ratios (preference score) of PBS/LPS-injected mice for B6, Trpc2$^{-/-}$, cGαi2$^{-/-}$, and V1rab$^{-/-}$ mice and their heterozygous controls. **b** B6 males (mean ± SEM, $n = 11$). **c** Trpc2$^{+/-}$ vs. Trpc2$^{-/-}$ males ($n = 9$, each). **d** Gαi2$^{+/-}$ vs. cGαi2$^{-/-}$ males ($n = 10$, 14, respectively). **e** V1rab$^{+/-}$ vs. V1rab$^{-/-}$ males ($n = 10$, 12, respectively). Unpaired *t*-tests, *$p < 0.05$, **$p < 0.01$, ***$p < 0.001$. ns, not significant $p = 0.06$–0.94. Open circles represent individual mice

time (IT) ratio = 0.81 ± 0.27, one-sample t-test: $p < 0.05$) (Fig. 1b). Next, we examined mice with a constitutive knockout of *Trpc2* (Trpc2$^{-/-}$) vs. heterozygous control mice (Trpc2$^{+/-}$) [33]. Trpc2$^{-/-}$ mice failed to display a preference for the healthy animal (PBS: 26.6 ± 3.5 s, LPS: 41.9 ± 5.2 s; $\log_2$ IT ratio = −0.64 ± 0.17), in contrast to their heterozygous littermate controls (PBS: 31.6 ± 3.4 s, LPS: 20.6 ± 2.6 s, $p < 0.05$; $\log_2$ IT ratio = 0.51 ± 0.22, $p < 0.001$) (Fig. 1c). Thus, Trpc2 is required for the lack of preference or avoidance of LPS-treated mice, results that are consistent with previous observations [3].

Trpc2 not only mediates signal transduction in VSNs but also in subsets of sensory neurons located in the main olfactory epithelium (MOE) [26, 27], making constitutive *Trpc2* knockout mice a much more complicated genetic model than previously anticipated. In fact, *Trpc2* is also required for avoidance behavior triggered by these MOE cells [26, 27]. It was, therefore, necessary to employ an alternative genetic strategy for dissecting innate avoidance of LPS-treated mice. We hypothesized that the LPS-dependent olfactory cues could be of low molecular weight (LMW) and, therefore, focused on the Gαi2-expressing (Gαi2^{+}) VSNs. For these experiments, we employed mice carrying an olfactory marker protein (*Omp-Cre*)-driven conditional knockout of Gαi2 (gene name: *Gnai2*) [14, 28, 29]. These mice are referred to as cGαi2 mice.

We found that, closely similar to Trpc2$^{-/-}$ mice, cGαi2$^{-/-}$ mice failed to show a preference for PBS-treated conspecifics, but rather displayed higher investigation times for the LPS-injected animals (Fig. 1d) (cGαi2$^{+/-}$- PBS: 58.4 ± 9.1 s, LPS: 33.0 ± 3.9 s, $p < 0.05$; cGαi2$^{-/-}$- PBS: 48.5 ± 4.7 s, LPS: 66.3 ± 6.9 s, $p = 0.06$; $\log_2$ IT ratio cGαi2$^{+/-}$ = 0.69 ± 0.18, cGαi2$^{-/-}$- $\log_2$ IT ratio = −0.47 ± 0.21, $p < 0.001$). Hence, the conditional *Omp-Cre*-driven Gαi2 deletion virtually phenocopied the effects of the global *Trpc2* deletion in the avoidance behavior of LPS-treated conspecifics. These results indicate that Gαi2 and Gαi2^{+} cells are required for mediating the chemosensory responses leading to the avoidance of conspecifics in an acute inflammatory state.

Gαi2^{+} VSNs of the apical layer of the VNE express >240 individual V1 receptor genes, classified into 12 subfamilies (families A-L), as well as 4 formyl peptide receptors (FPRs) [12, 34, 35]. To narrow down the VSN identities potentially involved in the avoidance of sick conspecifics,

we next tested mice harboring a cluster gene deletion of 16 V1Rs (V1rab$^{-/-}$) of the A and B families, which represent ~7% of all V1Rs [36]. We found that both V1rab$^{-/-}$ mice and V1rab$^{+/-}$ littermate controls displayed a clear preference for healthy mice (V1rab$^{+/-}$- PBS: 38.4 ± 4.4 s, LPS: 25.3 ± 3.1 s, $p < 0.05$; V1rab$^{-/-}$- PBS: 31.8 ± 3.2 s, LPS: 21.6 ± 2.9 s, $p < 0.05$; preference score: 0.63 ± 0.17 and 0.61 ± 0.17, respectively, $p = 0.94$) (Fig. 1e). Thus, these 16 V1R receptors are not essential in the avoidance of LPS-treated mice.

LPS-urine drives Gαi2-dependent avoidance and is detected by Gαi2$^+$ VSNs in freely behaving mice

LPS-dependent aversive chemosensory cues are present in the urine fraction of LPS-treated mice [3]. We next asked whether the avoidance, or lack of preference, for urine from LPS-treated mice also requires Gαi2. We tested olfactory preference of cGαi2$^{-/-}$ mice vs. cGαi2$^{+/-}$ mice to urine from PBS- or LPS-treated males using a two-choice test. We placed filter papers containing 50 µl of urine from LPS- or PBS-treated males in each lateral compartment of a three-chamber apparatus (Fig. 2a) and analyzed the time spent sniffing each odor source. LPS-urine did not elicit any avoidance in cGαi2$^{-/-}$ mice (PBS: 12.91 ± 1.54 s, LPS: 14.8 ± 2.3 s, $p = 0.49$; preference score: −0.08 ± 0.20), in contrast to cGαi2$^{+/-}$ control animals (PBS: 14.5 ± 1.9 s, LPS: 8.7 ± 1.9 s, $p < 0.05$; preference score: 0.67 ± 0.22, $p < 0.05$) (Fig. 2b, c). Analyses of each mouse showed that the majority (11/15) of cGαi2$^{+/-}$ control animals spent more time investigating PBS-urine, whereas only 6/16 cGαi2$^{-/-}$ mice showed a preference for PBS-urine vs. LPS-urine (Fig. 2d). These results reveal that urine from LPS-treated mice is less attractive in a two-choice test and that the preference for healthy urine requires Gαi2 signaling.

Can LPS-urine activate specific subsets of VSNs in freely behaving mice under in vivo conditions? To address this question, we analyzed VNO activation using immunodetection of the phosphorylated state of the 40S ribosomal protein S6 (pS6) as a proxy of cellular activation [37, 38] after exposing freely moving cGαi2$^{+/-}$ and cGαi2$^{-/-}$ mice to LPS-urine. Exposure to LPS-urine induced pS6 expression in 2.19% of VSNs in cGαi2$^{+/-}$ control mice (Fig. 2e, f). Importantly, the number of pS6-expressing cells was reduced by 55% in the VNO of cGαi2$^{-/-}$ mice after exposure to LPS-urine (0.98%, $p < 0.05$) (Fig. 2f). These results provide evidence that a substantial fraction of LPS-urine is detected by Gαi2$^+$ VSNs.

To validate these observations, we also analyzed the expression of the activity-driven c-Fos protein in cells of the accessory olfactory bulb (AOB), the brain structure targeted by VSN axonal projections. Stimulation with LPS-urine induced a significant increase in c-Fos expression in cGαi2$^{+/-}$ but not in cGαi2$^{-/-}$ mice when compared to unstimulated animals ($p < 0.01$). We analyzed the density of c-Fos-positive (c-Fos$^+$) cells following LPS-urine exposure in the anteroposterior AOB and observed significantly less c-Fos$^+$ cells in the anterior AOB of cGαi2$^{-/-}$ mice vs. cGαi2$^{+/-}$ mice (Fig. 2g; $p < 0.05$). In the posterior AOB, which receives sensory input from Gαo$^+$ VSNs, LPS-urine exposure did not induce any significant difference ($p = 0.21$), similar to unstimulated animals (Fig. 2g and Additional file 1: Suppl. Fig. 1). Taken together, these combined results provide strong evidence that exposure to LPS-urine leads to the in vivo activation of the Gαi2$^+$ vomeronasal subsystem.

Selective VSN Ca^{2+} responses to PBS- and LPS-urine require Gαi2

We next analyzed the selectivity and discrimination capabilities of native VSNs to LPS-urine vs. PBS-urine using dynamic Ca^{2+} imaging (Fig. 3). For this purpose, we employed *en face* imaging of individual dendritic endings (knobs) using a VNO whole-mount preparation that enables precise visualization of VSN activation patterns in response to chemostimulation [8, 13] and analyzed the density of activated knobs [8] (Fig. 3a). We loaded VSNs of cGαi2$^{+/-}$ and cGαi2$^{-/-}$ mice with the fluorescent Ca^{2+} indicator Rhod-2 and performed time-lapse confocal imaging. The surface of the VNE showed efficient loading of the vast majority of VSN dendritic knobs (Fig. 3b). Knob density was not statistically different between cGαi2$^{+/-}$ and cGαi2$^{-/-}$ VNEs (8.42 ± 0.3 and 8.21 ± 0.3 knobs/100 µm^2, respectively; $p = 0.61$) (Fig. 3c). Upon application of PBS- and LPS-urine at dilutions of 1:100,

(See figure on next page.)

Fig. 2 LPS-urine drives Gαi2-dependent avoidance and is detected by Gαi2$^+$ VSNs in freely behaving mice. **a** Three-chamber urine investigation assay where male mice could freely investigate filter papers treated with either urine from LPS- (LPS-urine; red) or PBS-treated males (PBS-urine; grey). Filter papers were placed in each lateral compartment. Bottom, examples of sniffing episodes of a control cGαi2$^{+/-}$ mouse and a cGαi2$^{-/-}$ mouse. **b** Investigation times of cGαi2$^{+/-}$ vs. cGαi2$^{-/-}$ mice to LPS-urine and PBS-urine ($n = 15$ and 16 respectively). **c** $\log_2$ investigation time ratios (preference score) of cGαi2$^{+/-}$ and cGαi2$^{-/-}$ mice to PBS-urine and LPS-urine ($n = 15$ cGαi2$^{+/-}$ and 16 cGαi2$^{-/-}$ mice). **d** Investigation time (preference above 50%) of individual cGαi2$^{+/-}$ and cGαi2$^{-/-}$ mice to PBS-urine or LPS-urine. **e** Representative images of activated VSNs (pS6, green) of cGαi2$^{+/-}$ and cGαi2$^{-/-}$ mice after exposure to LPS-urine. Nuclear DAPI staining in purple. Scale bar: 25 µm. **f** Percentage of pS6 positive cells in VNOs of cGαi2$^{+/-}$ and cGαi2$^{-/-}$ mice after exposure to LPS-urine (n = 6 cGαi2$^{+/-}$ and 5 cGαi2$^{-/-}$ mice). **g** Quantification of c-Fos$^+$ cells per µm^2 in the anterior and posterior AOB of cGαi2$^{+/-}$ and cGαi2$^{-/-}$ mice after exposure to LPS-urine ($n = 9$ cGαi2$^{+/-}$ and 7 cGαi2$^{-/-}$ mice). Mann-Whitney, *$p < 0.05$. Open circles represent individual mice

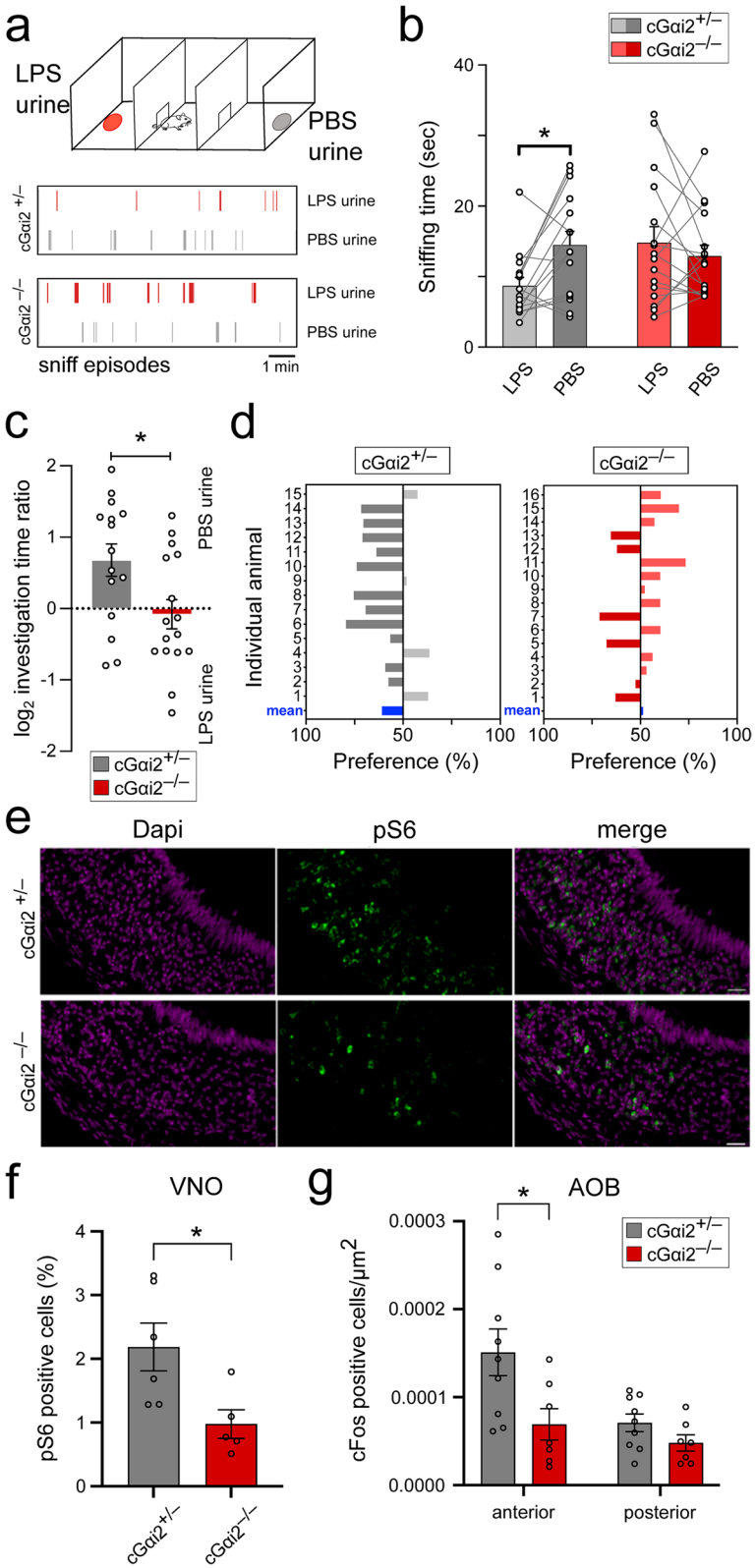

Fig. 2 (See legend on previous page.)

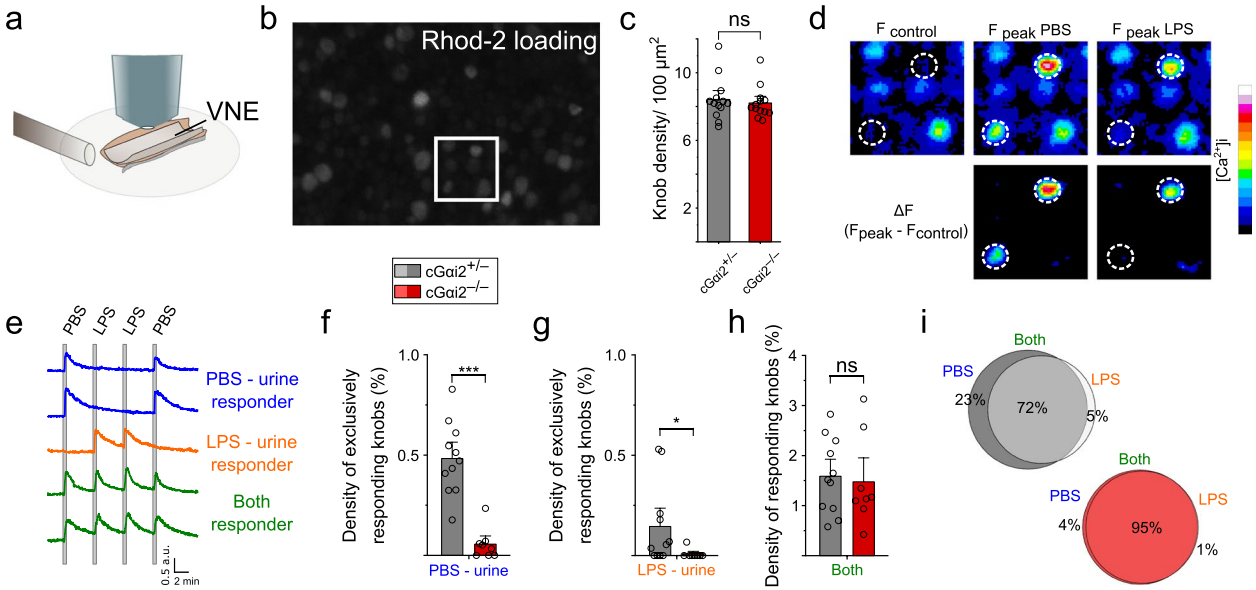

Fig. 3 VSN Ca^{2+} responses to LPS-urine require Gαi2. **a** *En face* VNE confocal Ca^{2+} imaging approach. **b** High magnification image of Rhod2/AM loaded vomeronasal knobs (100 × 60 µm). **c** Mean knob density does not differ in $cG\alpha i2^{+/-}$ vs. $cG\alpha i2^{-/-}$ VNOs ($n = 13$, each; Mann-Whitney: ns, $p = 0.61$). **d** Images showing Rhod-2 fluorescence at rest ($F_{control}$), at the peak of the response to male urine from PBS-treated mice (F_{peak} PBS), and at the peak of the response to male urine from LPS-treated mice (F_{peak} LPS). Bottom: ΔF images indicating responsive knobs to PBS- and/or LPS-urine (14 × 14 µm). **e** Example traces of confocal time-lapse recordings in single VSN dendritic knobs showing repeatable responses either to PBS-urine, to LPS-urine, or to both stimuli. **f** Density of knobs that responded to PBS-urine analyzed in control vs. $cG\alpha i2^{-/-}$ mice (11 and 8 recording sites in 6 and 5 animals, respectively; Mann-Whitney, $^{***}p < 0.001$). **g** Density of knobs that responded to LPS-urine analyzed in control vs. $cG\alpha i2^{-/-}$ mice (Mann-Whitney, $^{*}p < 0.05$). **h** Density of knobs that reacted to both PBS- and LPS-urine analyzed in control vs. $cG\alpha i2^{-/-}$ mice (unpaired *t*-test: $t\ (17) = 0.29$, $p = 0.77$). **i** Venn diagrams indicating the percentages of PBS- and LPS-urine responders and their overlap in control vs. $cG\alpha i2^{-/-}$ VNEs (based on 440 and 272 responding cells, respectively)

we observed synchronized and repeatable intracellular Ca^{2+} transients in numerous well-defined knobs (Fig. 3d). We analyzed 20,239 knobs (see the "Methods" section) in control VNOs and observed three different types of responses: (i) VSNs that were selectively activated by PBS-urine; (ii) VSNs that were selectively activated by LPS-urine; and (iii) VSNs that did not discriminate between both types of stimuli (Fig. 3d, e). Overall, both PBS- and LPS-urine activated a similar number of knobs (PBS-urine: 393 knobs, 2.1 ± 0.14%; LPS-urine: 340 knobs, 1.7 ± 0.25%) (Additional file 1: Suppl. Fig. 2a). These similarities suggest that the majority of knobs detect both stimuli. Indeed, of the responsive VSNs, 72% (1.6% of all knobs) detected both PBS- and LPS-urine, whereas only 23% (0.5% of all knobs) detected only PBS-urine, and 5% (0.1% of all knobs) detected only LPS-urine (Fig. 3f-i).

Next, we analyzed Ca^{2+} responses to PBS- or LPS-urine in $cG\alpha i2^{-/-}$ VNOs by imaging 18,269 individual knobs. There was a striking 10-fold reduction in the number of individual knobs that were activated selectively by PBS- or by LPS-urine (PBS-urine: 0.05 ± 0.03%; $p < 0.001$; LPS-urine: 0.01 ± 0.001%; $p < 0.05$) (Fig. 3f, g). The percentage of responders dropped from 23 to 4% for PBS-urine and from 5 to 1% for LPS-urine in control vs. $cG\alpha i2^{-/-}$ mice in this analysis (Fig. 3i). By contrast, the number of VSNs that detected both PBS- and LPS-urine remained closely similar between genotypes (1.6 ± 0.2% vs. 1.5 ± 0.3% of knobs; $p = 0.77$) (Fig. 3h), suggesting that this type of response is largely independent of Gαi2. Hence, these experiments indicate that conditional deletion of Gαi2 signaling in $cG\alpha i2^{-/-}$ mice leads to a dramatic reduction of cellular responses in those VSNs that are capable of discriminating PBS-urine vs. LPS-urine, and thus indicate that Gαi2 is required for this cellular discrimination.

Loss of Gαi2 predominantly impairs VSN Ca^{2+} responses to LMW urine fraction from healthy mice

To obtain direct evidence that the main activity of LPS-urine is contained in the LMW urine fraction, we used this LMW fraction (<10 kDa molecular mass) in our VSN Ca^{2+} imaging assay (Fig. 4). Chemicals present in this fraction are primarily detected by $G\alpha i2^{+}$ VSNs (~70%), but this fraction also contains small peptides and other molecules that are detected by $G\alpha o^{+}$ VSNs (30%) [14, 39, 40]. We recorded Ca^{2+} responses in 22,261 and 26,943 knobs from control and $cG\alpha i2^{-/-}$ VNOs, respectively,

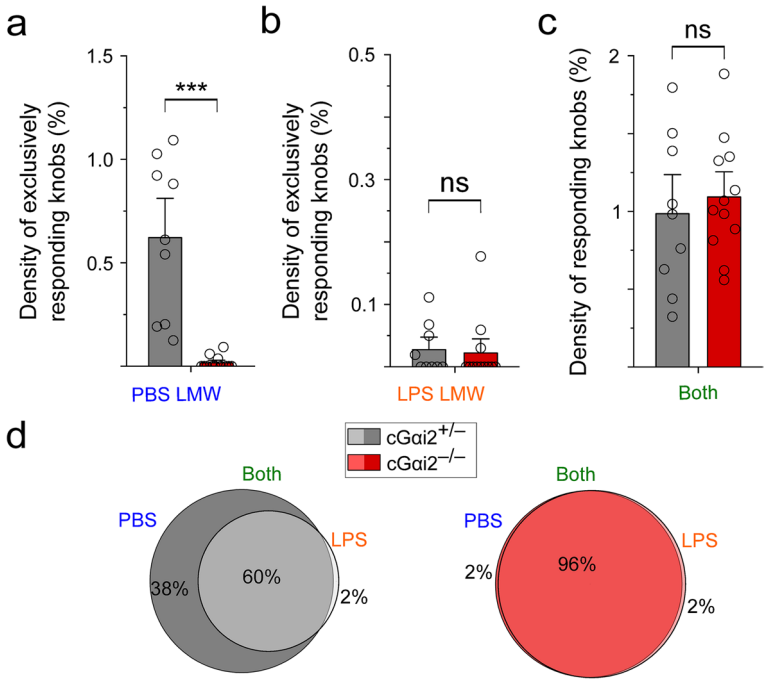

Fig. 4 Loss of Gαi2 predominantly impairs VSN Ca^{2+} responses to LMW urine fraction from healthy mice. **a**–**c** Density of knobs that responded to the LMW urine fraction of PBS- or LPS-treated mice analyzed in control vs. cGαi2$^{-/-}$ mice. **a** Density of knobs that responded exclusively to LMW_{PBS} (9 and 12 recording sites in 5 animals each, respectively; Mann-Whitney, ***$p < 0.001$). **b** Density of knobs that responded exclusively to LMW_{LPS} (Mann-Whitney ns, $p = 0.44$). **c** Density of knobs that responded to both LMW_{PBS} and LMW_{LPS} (unpaired *t*-test: $t\,(19) = 0.56$, $p = 0.58$). **d** Venn diagrams indicating the percentages of LMW_{PBS} and LMW_{LPS} responders and their overlap in control vs. cGαi2$^{-/-}$ knobs (based on 359 and 312 responding knobs, respectively)

and applied 1:100 dilutions of LMW_{PBS} and LMW_{LPS}. Overall, LMW_{PBS} and LMW_{LPS} activated a similar number of dendritic knobs (Additional file 1: Suppl. Fig. 2b), but there was a 33-fold reduction in the number of knobs that responded exclusively to LMW_{PBS} in cGαi2$^{-/-}$ VNOs (0.6 ± 0.12% vs. 0.018%; p < 0.001) (Fig. 4a). This VSN subpopulation represents 38% of LMW-activated knobs in control VNOs but only 2% in cGαi2$^{-/-}$ VNOs (Fig. 4d). By contrast, the number of knobs responding to LMW_{LPS} and those responding to both, $LMW_{PBS+LPS}$, were not significantly different in control vs. cGαi2$^{-/-}$ VNOs (LMW_{LPS}: 0.03 ± 0.01% vs. 0.02 ± 0.01%, $p = 0.44$; $LMW_{PBS+LPS}$: 1.00 ± 0.17% vs 1.1 ± 0.12%, $p = 0.58$) (Fig. 4b, c), suggesting that the differences observed with the whole LPS urine preparation (Fig. 3g) originated from molecules >10 kDa. Thus, conditional deletion of Gαi2 signaling predominantly reduced the number of VSNs capable of detecting chemosensory cues present in the LMW urine fraction from healthy mice.

VSN Ca^{2+} responses to feces extract from healthy and sick mice as well as to bile acids require Gαi2

Chemical stimuli such as bile acids are found in intestinal luminal contents (feces) and are known to be detected by VSNs [16, 41]. The abundance and nature of such chemicals could be affected in LPS-treated animals as these often show clear signs of diarrhea [42, 43]. We characterized VSN response profiles to feces by analyzing the Ca^{2+} responses of individual VSN dendritic knobs to feces extract (FE, diluted 1:100) from PBS- vs. LPS-injected mice. Similar to stimulation with urine, we found that FE from PBS- or LPS-treated mice could be discriminated by some VSNs whereas other cells reacted to both stimuli (Fig. 5a). In control mice, knobs were primarily activated by LPS-FE (96% of activated knobs), the majority of which (65%) responded exclusively to LPS-FE (Fig. 5c, f). Thus, the density of responding knobs to LPS-FE was 3-fold greater than to PBS-FE (Fig. 5e). Importantly, however, responses to both types of FE were nearly absent in cGαi2$^{-/-}$ VSNs (LPS-FE: 0.6 ± 0.09% vs. 0.004 ± 0.003%; $p < 0.001$; PBS-FE: 0.03 ± 0.02% vs. 0.01 ± 0.004%, $p = 0.25$; PBS-FE plus LPS-FE: 0.3 ± 0.05% vs. 0.036 ± 0.03%; $p < 0.01$) (Fig. 5b–e), indicating that Gαi2 is required for these responses.

We also analyzed VSN Ca^{2+} response profiles to two specific bile acids, cholic acid (CA, 10 µM) and deoxycholic acid (DCA, 10 µM) [16, 41]. Both molecules activated 1.1–1.5% of VSNs in control mice (Additional

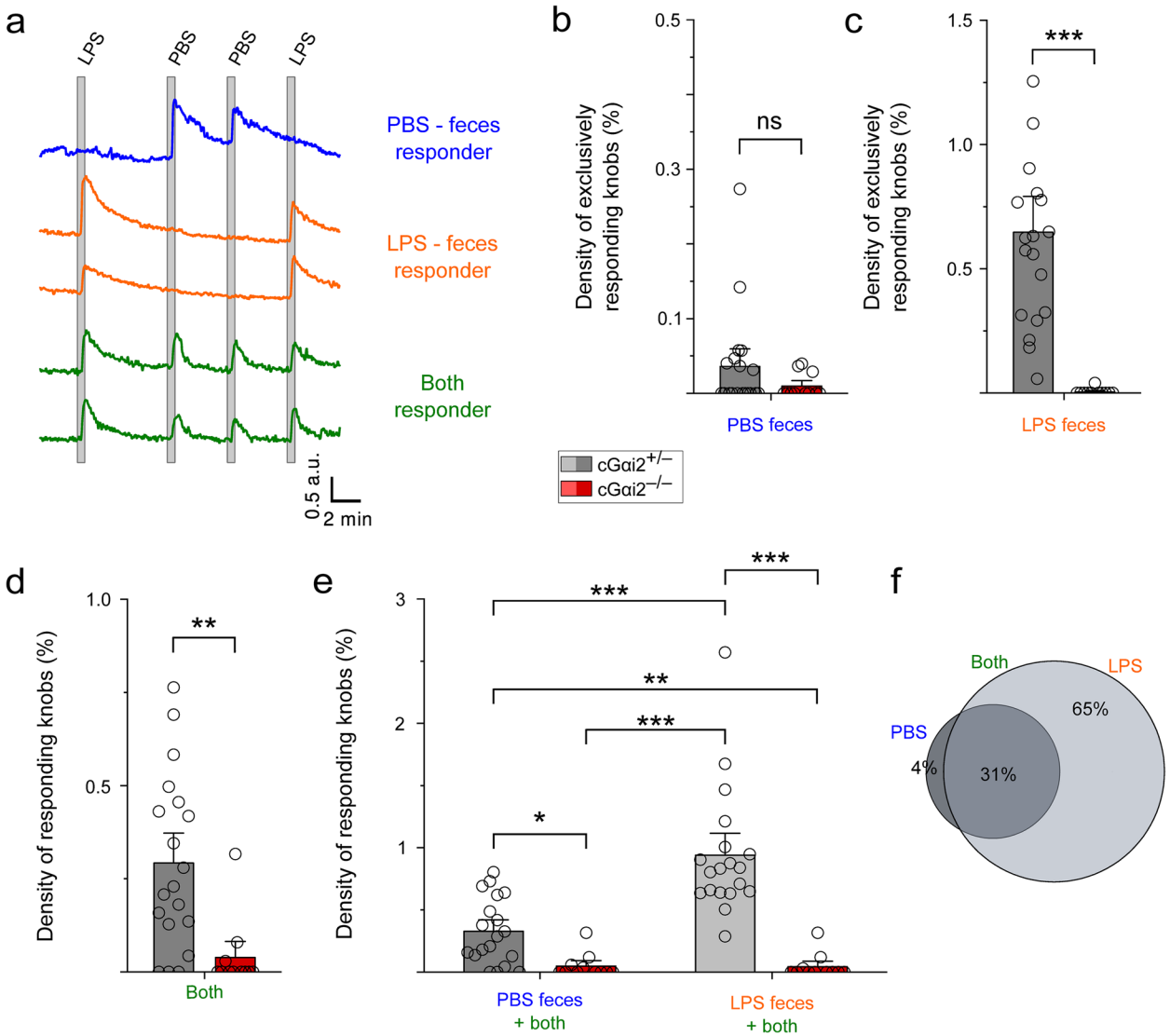

Fig. 5 VSN Ca^{2+} responses to feces extract (FE) from LPS- and PBS-treated mice require Gαi2. **a** Example traces of confocal time-lapse recordings in single VSN dendritic knobs showing repeatable responses to PBS-feces, to LPS-feces, or to both stimuli. **b**–**d** Density of knobs responding exclusively to FE solution from either PBS- or LPS-treated mice analyzed in control vs. cGαi2$^{-/-}$ VNEs. **b** Knobs that responded exclusively to PBS-feces in control vs. cGαi2$^{-/-}$ VNEs (19 and 11 recording sites in 10 and 5 animals, respectively; Mann-Whitney ns, $p = 0.25$). **c** Knobs that responded exclusively to LPS-feces (Mann-Whitney, ***$p < 0.001$). **d** Knobs that responded to both stimuli (Mann-Whitney, **$p < 0.01$). **e** Density of knobs that responded to PBS- and LPS-feces, either selectively or together ($n = 19$ and 11, respectively; Kruskal–Wallis ANOVA, $p < 0.001$; Mann-Whitney, *$p < 0.05$; ** $p < 0.01$; ***$p < 0.001$). **f** Venn diagram of response percentages to PBS- and LPS-feces in control knobs (based on 444 responding knobs)

file 1: Suppl. Fig. 3e), and 75% of FE-sensitive knobs also responded to CA/DCA (Additional file 1: Suppl. Fig. 3f). Here too, Ca^{2+} responses to CA or DCA were virtually absent in VSNs from cGαi2$^{-/-}$ VNOs (Additional file 1: Suppl. Fig. 3b-e). Together, these experiments show that FE from LPS-treated mice evokes altered response profiles in VSNs compared to FE from PBS-treated mice and that these effects are largely Gαi2-dependent. The results also show that VSN responses to two bile acids, CA and DCA, require Gαi2. We, therefore, considered these molecules as candidates to mediate the effects of LPS treatment on avoidance behavior.

Neither feces extract of LPS-treated mice nor bile acids induce avoidance behavior

We next tested whether FE from LPS-treated mice, like urine, is sufficient to induce avoidance behavior. We used healthy adult B6 males as stimulus animals

and painted their backs and anogenital regions with FE solution from either of two treatments. Stimulus animals were anesthetized and placed in different corners of a test arena (Fig. 6a). cGαi2$^{+/-}$ and cGαi2$^{-/-}$ test males were then introduced and allowed to freely investigate the stimulus animals for 10 min. Unexpectedly, neither cGαi2$^{+/-}$ nor cGαi2$^{-/-}$ males displayed any preference for any of the two conditions (Fig. 6b, c). Furthermore, healthy stimulus B6 mice swabbed with a mixture of two bile acids (CA and DCA, 10 µM each) also did not evoke any preference or avoidance behavior (Fig. 6d–f). Thus, unlike urine and despite being major activators of VSNs, neither FE (from PBS- or LPS-treated mice) nor the bile acids CA and DCA elicited any noticeable preference or avoidance behaviors in our assay. We conclude, therefore, that these types of stimuli can be ruled out in the search for the active compounds mediating inflammation-associated avoidance behavior of sick conspecific mice.

Information contained in LPS-urine and detected in a Gαi2-dependent manner is represented in multiple brain regions including the lateral habenula

Having shown that the representation of LPS-urine is initially processed across the olfactory periphery in the apical layer of VNO and anterior AOB and that these steps occur in a Gαi2-dependent manner (Fig. 2e, f, g), we next asked where in the CNS this information is encoded subsequently. We exposed cGαi2$^{+/-}$ vs. cGαi2$^{-/-}$ males to LPS-urine and analyzed the number of c-Fos^{+} cells in several brain areas including the posterodorsal and posteroventral medial amygdala (MeApd, MeApv), the dorsomedial subdivision of the ventromedial hypothalamus (VMHdm), the periaqueductal grey (PAG), and

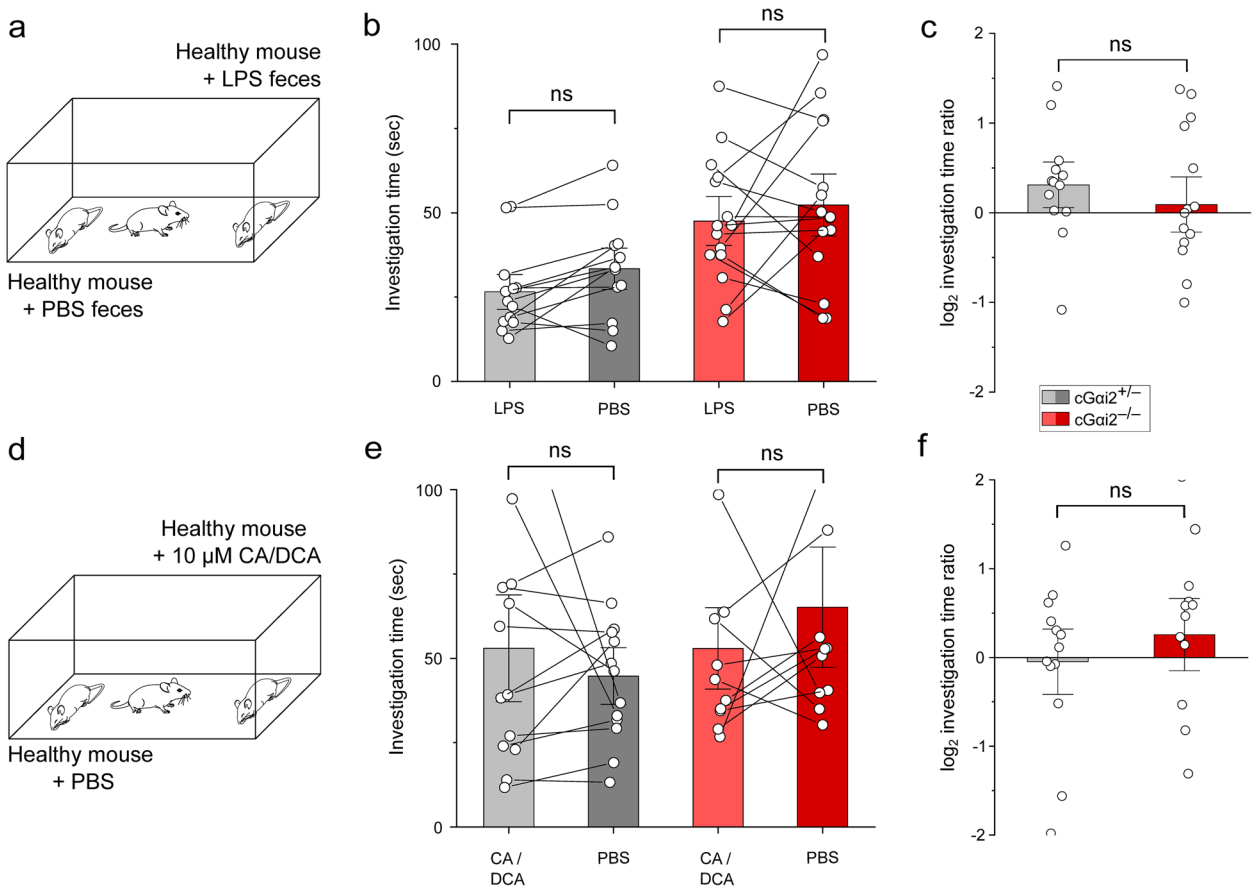

Fig. 6 Neither feces extract of LPS-treated mice nor bile acids induce avoidance behavior. **a** Conspecific investigation assay in which male mice were exposed to two healthy anesthetized males painted with FE solution of LPS- or PBS-treated males. **b** Investigation times of cGαi2$^{+/-}$ vs. cGαi2$^{-/-}$ mice (n = 13 and 15, respectively; cGαi2$^{+/-}$: unpaired t-test: t (24) = −1.29, p = 0.21, cGαi2$^{-/-}$: unpaired t-test: t (28) = −0.61, p = 0.55). **c** $\log_2$ investigation time ratios (preference score) (unpaired t-test: t (26) = −0.8, p = 0.43). **d** Male mice were allowed to investigate two healthy anesthetized male conspecifics painted with PBS solution supplemented with 10 µM CA + 10 µM DCA or with PBS alone. **e** Investigation times of healthy conspecifics painted with PBS or with PBS supplemented with CA/DCA in cGαi2$^{+/-}$ vs. cGαi2$^{-/-}$ mice (n = 13, 11, respectively; cGαi2$^{+/-}$: Mann-Whitney ns, p = 0.76, cGαi2$^{-/-}$: Mann-Whitney ns, p = 0.39). **f** $\log_2$ investigation time ratios (preference score) for healthy conspecifics painted with CA/DCA solution (unpaired t-test: t (22) = 0.83, p = 0.41)

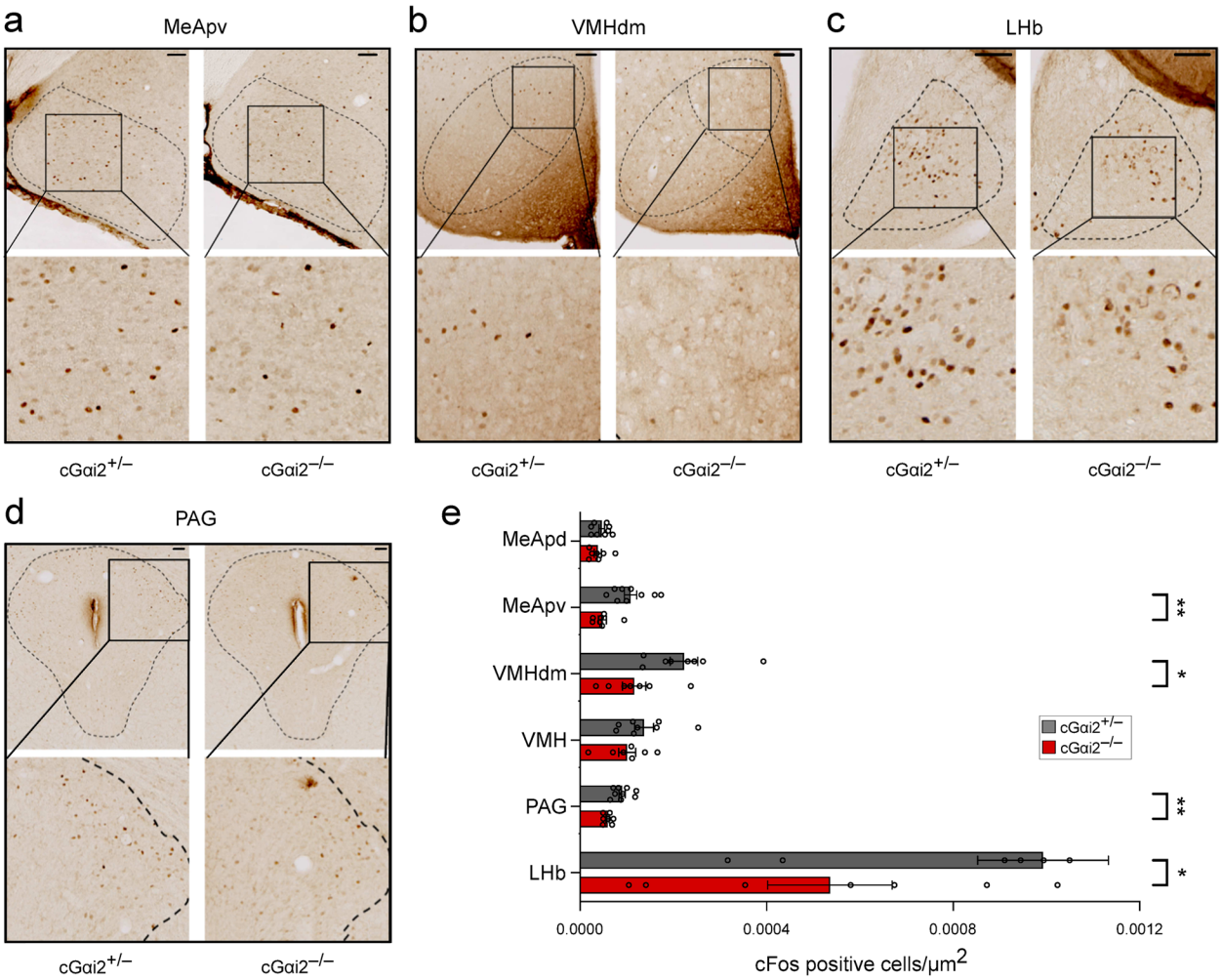

Fig. 7 Brain structures activated by LPS-urine. **a** Representative images of c-Fos activation in MeApv, **b** VMHdm, **c** LHb, and **d** PAG (areas delimitated by dashed lines) of cGαi2$^{+/-}$ and cGαi2$^{-/-}$ mice after exposure to LPS-urine. Bottom: higher magnification images of c-Fos^{+} cells. Scale bars: 50 µm. **e** Quantification of c-Fos^{+} cells per µm^{2} in MeApd, MeApv, VMHdm, VMH, PAG, and LHb of cGαi2$^{+/-}$ and cGαi2$^{-/-}$ mice after exposure to LPS-urine. Statistically significant reduction was observed in the MeApv, VMHdm, PAG, and LHb (n = 8-9 cGαi2$^{+/-}$ and 7 cGαi2$^{-/-}$ mice). No significant differences were observed in the VMH and MeApd (ns, p = 0.33–0.40). Mann-Whitney, *p < 0.05, **p < 0.01. Open circles represent individual mice

the lateral habenula (LHb) (Fig. 7 and Additional file 1: Suppl. Fig. 4a). Non-stimulated animals showed equivalent levels of basal c-Fos activity in all studied brain regions (Additional file 1: Suppl. Fig. 4a). Significantly, cGαi2-dependent c-Fos activation after stimulation with LPS-urine occurred in three major vomeronasal target regions: the MeApv, the VMHdm, and PAG (Fig. 7a–e). Notably, c-Fos activity induced by LPS-urine was lower in MeApd, MeApv, and PAG when compared to PBS-urine exposure in control animals (Additional file 1: Suppl. Fig. 4b). Interestingly, we also observed robust, cGαi2-dependent activation in the LHb (Fig. 7c, e), a structure that is activated by primary aversive stimuli [44]. In contrast to other areas, in the LHb, LPS-urine induced stronger c-Fos activation (4-fold increase) when compared to PBS-urine in control animals (Additional file 1: Suppl. Fig. 4c). Other areas of the medial amygdala and ventromedial hypothalamus lacked significant effects of the disruption of Gαi2 signaling (Fig. 7e).

Together, these results indicate that inflammation-associated odor information contained in conspecific LPS-urine must ultimately target and engage the MeApv, VMHdm, PAG, and LHb, and requires intact Gαi2 vomeronasal function.

Discussion

This study provides new insights into the full range of cellular and molecular parameters underlying the sensing and avoiding of sick conspecifics in mice. As such, this work confirms and extends a previous investigation

on this topic [3]. Several new results emerge from our work: (1) The demonstration that the G protein Gαi2 and the Gαi2$^+$ population of VSNs are required for the sensing and avoidance of conspecific mice that are in an acute state of inflammation; (2) the demonstration that conditional deletion of Gαi2 in the olfactory system phenocopies the effect of a constitutive *Trpc2* knockout with regard to sick conspecific avoidance, and that a cluster deletion of 16 V1Rs has no impact on avoidance of LPS-treated conspecifics; (3) the finding that the active components underlying the sensing of LPS-injected mice are contained in the urine fraction, but not in feces; (4) the result that two selected bile acids require Gαi2 for VSN activation but do not mimic the effects of LPS-urine on avoidance behavior; (5) the detailed analysis of dynamic Ca^{2+} responses in individual VSN dendritic knobs, that these cells can discriminate LPS- and PBS-urine and its LMW fraction, and how this discrimination depends on Gαi2; (6) the demonstration that the sensing and avoidance of sick conspecifics engages, in a Gαi2-dependent manner, the activation of multiple brain areas including the medial amygdala, the ventromedial hypothalamus, the periaqueductal grey, and the lateral habenula.

Rodents display a variety of behaviors and strategies, including chemosensation mediated by the accessory olfactory system, in order to avoid conspecifics that show signs of pathogen infection [3, 45, 46]. Our results demonstrate that the Gαi2$^+$ population of VSNs controls important features of sick conspecific discrimination. Specifically, we found that conditional deletion of Gαi2 suppresses preference behavior for healthy mice, consistent with a direct role of Gαi2 in the detection of an acute inflammatory state in conspecifics induced by LPS injection. Apical Gαi2 VSN subpopulations express ~240 V1Rs and 4 FPRs [35]. The precise identities of the specific receptors involved in the detection of chemosensory cues from sick conspecifics are unknown and remain to be investigated in future work, but our results employing a mouse line with a V1R cluster deletion [36] at least exclude the involvement of the type A and B subfamilies of V1Rs.

Excretions like urine and feces have been proposed as potential sources of odors specific to sick individuals [3, 45, 47]. Consistent with this, we observed that urine from LPS-injected mice is less attractive to healthy animals and that this preference requires Gαi2 signaling. Furthermore, analysis of sensory activity in the VSN dendritic knob layer shows that responses specific to urine from sick or healthy animals are preferentially detected by Gαi2$^+$ VSNs. This result is consistent with metabolomic characterizations of urine samples in states of inflammation that reported increases as well as decreases in volatile compounds, including V1R-specific ligands [48, 49]. Thus, the lack of preference for urine from sick animals may be caused by either a decrease in attractive olfactory signals or by the presence of repulsive cues in the urine. In this context, we have observed a greater number of specific VSN responses and increased c-Fos activity in the MeA and PAG in response to urine from healthy animals, indicating that an acute inflammatory state could lead to a loss or reduction of vomeronasal signaling. Moreover, specific responses to LMW urine fraction of healthy animals were strongly reduced in Gαi2 mutants, suggesting a possible role of the decrease of attractive cues after LPS injection. Further research will be needed to validate these possibilities. Importantly, we observed that application of LPS-feces extract nearly tripled the number of stimulated VSNs, indicating that treatment with LPS resulted in an increase of VNO ligands in feces, likely through changes in bile acid metabolism [50, 51]. Indeed, we identified two bile acids, CA and DCA, whose activity added up to approximately 75% of the feces-sensitive VSNs in a Gαi2-dependent manner. Although this is consistent with previous results linking the detection of feces and bile acids to V1Rs [16, 41], neither feces extract (LPS- or PBS-treated) nor the bile acids tested here were sufficient to induce an avoidance behavior, leading us to conclude that neither of these stimuli plays a critical role in the sensing and avoidance of LPS-treated mice.

Our c-Fos mapping results indicate that the representation of LPS-urine in the CNS involves several downstream brain areas of the Gαi2 vomeronasal pathway: AOB, MeApv, VMHdm, and PAG. These results are consistent with a number of studies implicating these brain areas in defensive, avoidance, and escape behaviors, including avoidance to predator odors [25, 52–55]. Remarkably, stimulation with LPS-urine induced fewer c-Fos$^+$ cells in MeA and PAG as compared with PBS-urine in control animals, which is consistent with the higher sensory activity observed in VSN dendritic knobs in response to specific PBS- vs LPS-urine signals. By contrast, we observed greater Gαi2-dependent c-Fos activity by LPS-urine in the LHb, a phylogenetically ancient brain region that is activated by aversive stimuli and modulates conspecific interactions [44, 56]. The LHb receives inputs from limbic structures and targets midbrain neuromodulatory systems, such as the dopaminergic and serotonergic systems, underlying negative emotional states and negative reward [57]. To the best of our knowledge, these are the first results to implicate the lateral habenula in the sensing and avoidance of chemosensory cues associated with conspecifics that are in acute inflammatory state.

Conclusions

In summary, our results indicate that the sensing and avoidance of LPS-treated sick conspecifics critically depend on the Gαi2$^+$ vomeronasal subsystem. In

particular, our observations point to a central role of brain circuits downstream of the olfactory periphery in the AOB, MeApv, VMHdm, PAG, and LHb in the control of sick conspecific avoidance. Our results are consistent with studies implicating the MePV and VMHdm in defensive, escape, and avoidance behaviors and the LHb in negative reward prediction in aversive learning. By identifying specific molecular properties of the sensory neurons that mediate sick conspecific discrimination, we have provided new insights into the genetic substrates and circuit logic of the sensing of inflammation in mice. These results should facilitate further studies aimed at understanding the active chemicals, their receptors, and the neural circuits underlying the perception of sickness by conspecifics.

Methods

Mice

Experiments were performed on adult, 8–20-week-old male mice. We employed the following genotypes: (1) Wild-type mice (C57BL/6N, denoted as B6) were obtained from Charles River Laboratories (Sulzfeld, Germany). (2) Mice harboring a targeted, global deletion of the *Trpc2* gene (B6;129P2-Trpc2 < tm2Mom > / MomJ, Stock# 006733; RRID:IMSR_JAX:006733; denoted as $Trpc2^{-/-}$ mice) [33]. (3) Conditional Gαi2 knockout mice (denoted as $cG\alpha i2^{-/-}$) harboring a Cre recombinase-mediated ablation of the *Gnai2* gene under the control of the olfactory marker protein (*Omp*) promoter and generated as described [14]. Mice were homozygous for the floxed *Gnai2* alleles and heterozygous for Cre and *Omp* ($Gnai2^{fx/fx}$ $Omp^{cre/+}$ or $cG\alpha i2^{-/-}$). In these mice, Cre-mediated *Gnai2* deletion was restricted to *Omp*-positive cells. Animals heterozygous for both alleles ($Gnai2^{fx/+}$ $Omp^{cre/+}$ or $cG\alpha i2^{+/-}$) or homozygous $Gnai2^{+/+}$ $Omp^{+/+}$ ($cG\alpha i2^{+/+}$) served as controls. (4) Mice harboring a targeted, global deletion of 16 intact V1r genes of families A and B (129S-Del(6)1Mom/MomJ, RRID:IMSR_JAX:006653, common name ΔV1rabΔ, denoted as $V1rab^{-/-}$ [36]. Control mice were heterozygous littermates. Mice were housed in individually ventilated cages (IVCs) on a 12:12-h light-dark cycle with food and water available *ad libitum*.

Treatment of mice with LPS and urine and feces collection

Male mice (B6, 8–20 weeks old) were injected intraperitoneally with 1–5 mg/kg LPS (Lipopolysaccharide L4516 and L4391, Sigma, in 200 µl phosphate-buffered saline, PBS) depending on the endotoxin units (EU) according to the specification sheet of the Lot (3,000,000 EU/kg). Control mice received 200 µl PBS injections. Mice were returned into their individual home cages and were used as stimulus animals 4 h post-injection. Urine and feces from several mice injected with LPS or PBS were collected (4 h post-injection), pooled and stored at −80 °C until use. To obtain urine fractions, 0.5 ml of PBS- or LPS-urine was size-fractionated by centrifugation (14,000 × g for 30 min) using Nanosep (Pall) 10-kDa molecular mass cutoff ultrafiltration columns. The centrifugation supernatant was the LMW fraction (<10 kDa). Feces was diluted 1:10 (w:v) in water, vortexed, and left overnight on a shaker at 4° C. The suspension was then centrifuged two times at 2400×*g* for 20 min. The supernatant was aliquoted and stored at −80 °C until use. To measure rectal temperature of the injected animals, mice were placed on a horizontal surface, e.g., a cage lid. The tail was then lifted, and a probe of a fast-acquiring thermometer (<1 s, DTM light, LKM electronic, Geraberg) was gently inserted into the rectum.

VNO whole-mount preparation and *en face* Ca^{2+} imaging

Mice were deeply anesthetized with CO_2, sacrificed by decapitation, and VNOs were rapidly removed and dissected in ice-cold oxygenated (95% O_2, 5% CO_2) S1 solution containing (in mM) 120 NaCl, 25 $NaHCO_3$, 5 KCl, 5 N,N-bis(2-hydroxyethyl)-2-aminoethanesulfonic acid (BES), 1 $MgSO_4$, 1 $CaCl_2$, 10 glucose, and pH 7.3 (osmolarity: 300 mOsm/l). One half of the VNO within the bony capsule was glued (Loctite 401) to a petri dish (Ø 4 cm), the bony capsule was opened with fine forceps, and the non-sensory tissue was stripped off to expose the VNE to gain access to the surface of the VSN dendritic knobs. Tissue and cell debris as well as the posterior vomeronasal glands were removed and the *en face* preparation was then loaded with Rhod-2/AM (15 µM) calcium dye. Loading was performed at room temperature in carbogenated S1 solution for 1 h. Rhod-2 solution was then removed, and the petri dish was placed on an upright confocal laser scanning microscope (Leica TCS SP5 II, 20× water immersion objective HCX APO L20×/1.0w) equipped with Ar and He/Ne lasers. Rhod-2 was excited at 543 nm, emission was measured between 560 and 680 nm. Images were collected every 1.5 s (1024 × 1024). Stimuli were applied to the VNO surface using a local perfusion system which produced a continuous solution stream (Fig. 3a). All stimuli were diluted in S1 solution and applied for 30 s at least twice during an experiment. Interstimulus interval was at least 4 min. We used urine (1:100 dilution), LMW fraction urine (1:100), and feces solution (1:100) from PBS- or LPS-injected B6 males (see the "Treatment of mice with LPS and urine and feces collection" section). Stock solutions of cholic acid (CA) and deoxycholic acid (DCA) were prepared in methanol and ethanol, respectively, and stored at 4° C. Final solutions (10 µM each) were prepared immediately before use in oxygenated S1 solution. All physiological

measurements were performed at room temperature. Data analysis was performed with ImageJ (NIH). Time series stacks were aligned using the Template Matching plugin. Ca^{2+} responses of individual dendritic knobs were normalized to the knob resting fluorescence level obtained before stimulation (ratio Fx/F0, Fx = actual fluorescence; F0 = mean fluorescence of the first 50 images of the experiment). The following criteria for stimulus-induced Ca^{2+} responses were applied. (i) A response was defined as a stimulus-dependent deviation of fluorescence that exceeded twice the SD of the mean of the baseline fluorescence noise. (ii) A response had to occur within 1 min after stimulus application. (iii) Knobs were considered responsive if they reacted to a given stimulus during both applications. For calculation of VSN knob density, we analyzed randomly selected VNO regions (40 × 40 µm) in 13 recorded areas of cGαi2$^{+/-}$ and cGαi2$^{-/-}$ VNOs and counted knob-like structures. The mean density was 8.42 ± 0.35 and 8.21 ± 0.26 knobs/100 µm^2, respectively. The mean density of all analyzed areas (cGαi2$^{+/-}$ and cGαi2$^{-/-}$) of 8.32 knobs/100 µm^2 was used to calculate the total knob number in the recorded area. Sampling areas comprised ~13,000 to ~ 40,000 µm^2 per experiment leading to calculated knob numbers of ~1100 to ~3300 knobs. The number of responding knobs was then quantified in relation to sample area and thus calculated total knob number [8].

Behavioral testing

All behavioral tests were conducted with adult (8–20-week-old) test and stimulus animals. Habituation and tests were always conducted during the dark phase in a behavior room under infrared light conditions (21 °C, humidity >40%). Experiments were digitally recorded and subsequently analyzed by a blind experimenter.

Conspecific investigation

We tested preference by giving adult male mice of various genotypes a choice to freely investigate two types of stimulus animals: PBS- vs. LPS-injected anesthetized B6 mice. Test mice were habituated for 2–3 days (for 10 min each day) by introducing cage mates (2–3 mice / cage) into an empty type II cage (floor area 32 × 16 cm) that was secured by a Plexiglas attachment. After 10 min, mice were returned to their home cages. On testing days, stimulus mice (4 h post-injection with either LPS or PBS) were anesthetized with 100 mg/kg ketamine (Serumwerk Bernburg, Bernburg, Germany) and 8 mg/kg xylazine (Serumwerk Bernburg, Bernburg, Germany) and placed on opposite sides of a neutral empty cage. We also tested the preference by adult male cGαi2 mice to freely investigate two types of stimulus mice: (1) healthy anesthetized B6 mice painted with 70 µl feces solution of LPS- or PBS-injected stimulus mice at the anogenital region and back; (2) healthy anesthetized B6 mice painted with PBS solution supplemented with CA/DCA (10 µM each) or PBS solution alone (70 µl) at the anogenital region and back. The test mouse was placed between the two stimulus mice and recorded for 10 min with an infrared digital video camera. All mice showed a keen interest in investigating the stimulus source during which their nose was in close contact with the stimulus animals. Investigative behavior was scored manually using Behavioral Observation Research Interactive Software (BORIS) [58]. Stimulus mice were used in several consecutive trials. We did not observe any influence of trial number on investigation times. The avoidance index was calculated as $\log_2$ investigation time ratio = $\log_2$ IT_{PBS}/IT_{LPS}, with IT_{PBS} as the time a mouse investigated the PBS stimulus animal and IT_{LPS} as the time a mouse investigated the LPS stimulus mouse. Negative values represent preference for the LPS-treated stimulus animal and positive values represent preference for the PBS-treated stimulus animal.

Urine investigation assay

Two days before a test, mice were daily habituated to the three chambers box for 10 min with unscented stimuli in each side chamber. On the test day, 50 µl of urine from LPS-treated and PBS-treated males were placed on filter papers in each lateral compartment. The sides containing the stimuli were randomized, and the apparatus was cleaned with 20% ethanol between subjects. Mice were free to investigate the apparatus for 10 min. The time spent in each chamber and the duration of chemosensory investigation were scored and an avoidance index calculated as described above.

Immunostaining

Tissue preparation

Mice were individually housed for at least 4 days and exposed to either a clean filter paper, or a filter paper with 50 µl of LPS-treated male urine. Ninety minutes after continuous exposure, mice were anesthetized by an overdose of pentobarbital (Ceva) and perfused transcardially with 0.9% saline solution followed by 0.1 M phosphate buffer (PB) containing 4% paraformaldehyde (PFA). Brains and VNOs were removed, postfixed overnight in 4% PFA, and cryoprotected in 0.1 M PB containing 30% sucrose. Brains, VNOs and olfactory bulbs (OB) were embedded separately in Tissue-Tek® O.C.T™ compound, snap-frozen in cold isopentane, and processed on a Leica CM 3050S cryostat. Brain samples were cut in 30-µm serial free-floating sections (coronal for brains, sagittal for OB) using tris-buffered saline solution (TBS) containing 0.1% sodium azide. VNOs were cut in 16-µm serial

coronal sections and directly mounted on SuperFrost Plus slides.

pS6 immunolabeling

Slides were washed (3 × 5 min) in TBS, incubated in blocking solution (TBS containing 0.3% Triton X-100, TBS-T, and 2% donkey serum) 2 h at room temperature (RT), and overnight at 4 °C in blocking solution supplemented with the pS6 primary antibody (1:2500; rabbit polyclonal #44-923G, Invitrogen). Slides were then washed in TBS and incubated in TBS-T supplemented with secondary antibody (1:1000 Cy3-conjugated donkey anti-rabbit IgG, Jackson ImmunoResearch) for 2 h at RT. Nuclei were counterstained 5 min at RT with DAPI. Slides were mounted with Fluoromount-G™ (Invitrogen).

c-Fos immunolabeling

Sections were washed (3 × 5 min) in TBS; endogenous peroxidases were blocked for 30 min in TBS containing 3% H_2O_2. Sections were incubated in blocking solution (TBS containing 0.1% Triton X-100, TBS-T, and 5% normal goat serum) 2 h at RT, and then overnight at 4 °C in blocking solution supplemented with the c-Fos primary antibody (1:1000 mouse monoclonal #sc271243, Santa Cruz Biotechnology). Sections were then washed in TBS and incubated in TBS-T supplemented with secondary antibody (1:1000; biotinylated goat anti-mouse IgG, Jackson ImmunoResearch) for 2 h at RT. Signals were amplified with VECTASTAIN® ABC kit (Vector) for 1 h at RT and then visualized with diaminobenzidine (DAB 0,02%, 0,01% H_2O_2 in 0,05 M Tris, pH 7,4). Slides were mounted with DPX (Sigma-Aldrich).

Analysis

For c-Fos experiments, slides were scanned using an automatic slide scanner (Axio Scan.Z1, Zeiss). Regions of interest were drawn from scanned brain sections based on the Paxinos mouse brain atlas using QuPath tools [59]. Coronal sections were selected for the LHb, 3–5 sections between bregma −1.22 mm and −1.70 mm; for MeA and VMH, 3–5 sections between bregma −1.34 mm and −1.70 mm; and for PAG, 3–6 sections between bregma −3.40 mm and −3.88 mm. The number of c-Fos$^+$ nuclei in each drawn region was automatically counted using the built-in Cell Detection method. The same cell detection parameters, such as set up, nucleus, and intensity parameters, were applied to all the regions. pS6-positive cells were counted using Zen software (blue edition 3.0, Zeiss) and the particle analyzer plug-in of Fiji [60] on 6–15 VNO images per animal and expressed as a proportion of the total DAPI-positive nuclei. For both c-Fos and pS6 measurements, a manual validation of all positive detected cells was performed before exporting all values.

Statistics

Statistical analyses were performed using the software Origin Pro 2021 (OriginLab Corporation, Northampton, MA, USA) and GraphPad Prism 9.0 (GraphPad Software). Assumptions of normality were tested before conducting the following statistical tests. Student's *t*-test was used to measure the significance of the differences between two distributions. In case the results failed the test of normality, Mann-Whitney test was performed. Multiple groups were compared using Kruskal-Wallis one-way analysis of variance (ANOVA) with Mann-Whitney and Holm-Šídák's tests as a post hoc comparison. The probability of error level (alpha) was chosen to be 0.05. The statistical tests used were two-sided. Unless otherwise stated, data are expressed as mean ± standard error of the mean (SEM). Specific statistics and number of samples analyzed are described in the figure captions.

Abbreviations

AOB	Accessory olfactory bulb
CA	Cholic acid
CNS	Central nervous system
DCA	Deoxycholic acid
FE	Feces extract
FPR	Formyl peptide receptor
IT	Investigation time
LHb	Lateral habenula
LMW	Low molecular weight
LPS	Lipopolysaccharide
MeApd	Posterodorsal medial amygdala
MeApv	Posteroventral medial amygdala
MOE	Main olfactory epithelium
OMP	Olfactory marker protein
PAG	Periaqueductal grey
PBS	Phosphate-buffered saline
pS6	40S ribosomal protein S6
V1R	Vomeronasal type 1 receptor
V2R	Vomeronasal type 2 receptor
VMH	Ventromedial hypothalamus
VMHdm	Dorsomedial subdivision of the ventromedial hypothalamus
VNO	Vomeronasal organ
VSNs	Vomeronasal sensory neurons

Supplementary Information

The online version contains supplementary material available at https://doi.org/10.1186/s12915-023-01653-8.

Additional file 1: Suppl. Fig. 1. No significant difference in c-Fos activation in anterior and posterior AOB of non-stimulated cGαi2$^{+/-}$ and cGαi2$^{-/-}$ mice. **Suppl. Fig. 2.** Overall, both PBS-and LPS-urine as well as LMW urine fractions activated a similar number of VSN dendritic knobs. **Suppl. Fig. 3.** VSN Ca^{2+} responses to two selected bile acids (CA and DCA) require Gαi2. **Suppl. Fig. 4.** No significant difference in c-Fos activation in brain regions of non-stimulated cGαi2$^{+/-}$ and cGαi2$^{-/-}$ mice.

Additional file 2: Dataset S1. Dataset containing values andstatistical analyses displayed in all the figures.

Acknowledgements

We thank Chantal Porte for technical assistance; Daniel Schauenburg, Kerstin Becker, Lisa-Marie Knieriemen, Deborah Crespin, and Aurelie Gasnier for mouse husbandry; Martina Pyrski for fruitful discussions; and Marie-Claire Blache for imaging experiments. Source of mouse silhouettes: https://scidraw.io/

Authors' contributions
PC and JW designed the research; JW, A-CT, and HV performed research; TL-Z contributed to methodology and resources; JW, A-CT, and HV analyzed data; PC, TL-Z, A-CT, and FZ provided funding acquisition; PC, FZ, and JW wrote the manuscript with edits from all authors. All authors read and approved the final manuscript.

Funding
This work was supported by Deutsche Forschungsgemeinschaft (DFG) grants Sonderforschungsbereich 894 project A17 (FZ and TL-Z) and Sonderforschungsbereich-Transregio TRR 152 project P10 (FZ and TL-Z), Agence National de la Recherche (ANR) grant ANR-20-CE92-0003 (PC), and Region Centre Val de Loire project 201900134883 (PC). A-CT was supported by a grant from the University of Tours and Region Centre Val de Loire.

Availability of data and materials
All data generated or analyzed during this study are included in this published article and its supplementary information files. Individual data values are provided in Additional File 2.

Declarations

Ethics approval and consent to participate
All procedures were approved by the Institutional Animal Care and Use Committee of Saarland University School of Medicine (approval numbers: CIPMM-2.2.4.1.1 and GB3-2.4.2.2.-02/2020) and were in accordance with the laws for animal experiments issued by the German and French Governments and approved by an ethical committee for animal experimentation (CEEA Val de Loire project 12785).

Consent for publication
Not applicable

Competing interests
The authors declare that they have no competing interests.

Author details
[1]Center for Integrative Physiology and Molecular Medicine, Saarland University, 66421 Homburg, Germany. [2]Laboratoire de Physiologie de la Reproduction et des Comportements, UMR 0085 INRAE-CNRS-IFCE-University of Tours, Nouzilly, France.

Received: 24 January 2023 Accepted: 23 June 2023
Published online: 10 July 2023

References

1. Kavaliers M, Choleris E, Agmo A, Pfaff DW. Olfactory-mediated parasite recognition and avoidance: linking genes to behavior. Horm Behav. 2004;46:272–83.
2. Kraus A, Buckley KM, Salinas I. Sensing the world and its dangers: an evolutionary perspective in neuroimmunology. Elife. 2021;10:e66706.
3. Boillat M, Challet L, Rossier D, Kan C, Carleton A, Rodriguez I. The vomeronasal system mediates sick conspecific avoidance. Curr Biol. 2015;25:251–5.
4. Brennan PA, Zufall F. Pheromonal communication in vertebrates. Nature. 2006;444:308–15.
5. Stowers L, Holy TE, Meister M, Dulac C, Koentges G. Loss of sex discrimination and male-male aggression in mice deficient for TRP2. Science. 2002;295:1493–500.
6. Leypold BG, Yu CR, Leinders-Zufall T, Kim MM, Zufall F, Axel R. Altered sexual and social behaviors in trp2 mutant mice. Proc Natl Acad Sci U S A. 2002;99:6376–81.
7. Papes F, Logan DW, Stowers L. The vomeronasal organ mediates interspecies defensive behaviors through detection of protein pheromone homologs. Cell. 2010;141:692–703.
8. Bufe B, Teuchert Y, Schmid A, Pyrski M, Perez-Gomez A, Eisenbeis J, et al. Bacterial MgrB peptide activates chemoreceptor Fpr3 in mouse accessory olfactory system and drives avoidance behaviour. Nat Commun. 2019;10:4889.
9. Liberles SD. Mammalian pheromones. Annu Rev Physiol. 2014;76:151–75.
10. Mohrhardt J, Nagel M, Fleck D, Ben-Shaul Y, Spehr M. Signal Detection and Coding in the Accessory Olfactory System. Chem Senses. 2018;43:667–95.
11. Jia C, Halpern M. Subclasses of vomeronasal receptor neurons: differential expression of G proteins (Gi alpha 2 and G(o alpha)) and segregated projections to the accessory olfactory bulb. Brain Res. 1996;719:117–28.
12. Liberles SD, Horowitz LF, Kuang D, Contos JJ, Wilson KL, Siltberg-Liberles J, et al. Formyl peptide receptors are candidate chemosensory receptors in the vomeronasal organ. Proc Natl Acad Sci U S A. 2009;106:9842–7.
13. Rivière S, Challet L, Fluegge D, Spehr M, Rodriguez I. Formyl peptide receptor-like proteins are a novel family of vomeronasal chemosensors. Nature. 2009;459:574–7.
14. Trouillet AC, Keller M, Weiss J, Leinders-Zufall T, Birnbaumer L, Zufall F, et al. Central role of G protein Gαi2 and Gαi2^{+} vomeronasal neurons in balancing territorial and infant-directed aggression of male mice. Proc Natl Acad Sci U S A. 2019;116:5135–43.
15. Chamero P, Katsoulidou V, Hendrix P, Bufe B, Roberts R, Matsunami H, et al. G protein Gαo is essential for vomeronasal function and aggressive behavior in mice. Proc Natl Acad Sci. 2011;108:12898–903.
16. Doyle WI, Dinser JA, Cansler HL, Zhang X, Dinh DD, Browder NS, et al. Faecal bile acids are natural ligands of the mouse accessory olfactory system. Nat Commun. 2016;7:11936.
17. Nodari F, Hsu FF, Fu X, Holekamp TF, Kao LF, Turk J, et al. Sulfated steroids as natural ligands of mouse pheromone-sensing neurons. J Neurosci. 2008;28:6407–18.
18. Isogai Y, Si S, Pont-Lezica L, Tan T, Kapoor V, Murthy VN, et al. Molecular organization of vomeronasal chemoreception. Nature. 2011;478:241–5.
19. Haga-Yamanaka S, Ma L, He J, Qiu Q, Lavis LD, Looger LL, et al. Integrated action of pheromone signals in promoting courtship behavior in male mice. Elife. 2014;3:e03025.
20. Fu X, Yan Y, Xu PS, Geerlof-Vidavsky I, Chong W, Gross ML, et al. A molecular code for identity in the vomeronasal system. Cell. 2015;163:313–23.
21. Haga S, Hattori T, Sato T, Sato K, Matsuda S, Kobayakawa R, et al. The male mouse pheromone ESP1 enhances female sexual receptive behaviour through a specific vomeronasal receptor. Nature. 2010;466:118–22.
22. Isogai Y, Wu Z, Love MI, Ahn MH, Bambah-Mukku D, Hua V, et al. Multisensory logic of infant-directed aggression by males. Cell. 2018;175(1827–41): e17.
23. Boillat M, Carleton A, Rodriguez I. From immune to olfactory expression: neofunctionalization of formyl peptide receptors. Cell Tissue Res. 2021;383:387–93.
24. Bufe B, Schumann T, Kappl R, Bogeski I, Kummerow C, Podgórska M, et al. Recognition of bacterial signal peptides by mammalian formyl peptide receptors: a new mechanism for sensing pathogens. J Biol Chem. 2015;290:7369–87.
25. Pérez-Gómez A, Bleymehl K, Stein B, Pyrski M, Birnbaumer L, Munger SD, et al. Innate predator odor aversion driven by parallel olfactory subsystems that converge in the ventromedial hypothalamus. Curr Biol. 2015;25:1340–6.
26. Bleymehl K, Pérez-Gómez A, Omura M, Moreno-Pérez A, Macías D, Bai Z, et al. A sensor for low environmental oxygen in the mouse main olfactory epithelium. Neuron. 2016;92:1196–203.
27. Koike K, Yoo SJ, Bleymehl K, Omura M, Zapiec B, Pyrski M, et al. Danger perception and stress response through an olfactory sensor for the bacterial metabolite hydrogen sulfide. Neuron. 2021;109:2469-84.e7.
28. Pallé A, Montero M, Fernández S, Tezanos P, de Las Heras JA, Luskey V, et al. Gαi2^{+} vomeronasal neurons govern the initial outcome of an acute social competition. Sci Rep. 2020;10:894.
29. Trouillet A-C, Moussu C, Poissenot K, Keller M, Birnbaumer L, Leinders-Zufall T, et al. Sensory detection by the vomeronasal organ modulates experience-dependent social behaviors in female mice. Front Cell Neurosci. 2021;15:638800.
30. Dantzer R, O'Connor JC, Freund GG, Johnson RW, Kelley KW. From inflammation to sickness and depression: when the immune system subjugates the brain. Nat Rev Neurosci. 2008;9:46–56.
31. Liman ER, Corey DP, Dulac C. TRP2: a candidate transduction channel for mammalian pheromone sensory signaling. Proc Natl Acad Sci U S A. 1999;96:5791–6.
32. Lucas P, Ukhanov K, Leinders-Zufall T, Zufall F. A diacylglycerol-gated cation channel in vomeronasal neuron dendrites is impaired in TRPC2

mutant mice: mechanism of pheromone transduction. Neuron. 2003;40:551–61.
33. Omura M, Mombaerts P. Trpc2-expressing sensory neurons in the main olfactory epithelium of the mouse. Cell Rep. 2014;8:583–95.
34. Miller CH, Campbell P, Sheehan MJ. Distinct evolutionary trajectories of V1R clades across mouse species. BMC Evol Biol. 2020;20:99.
35. Tirindelli R. Coding of pheromones by vomeronasal receptors. Cell Tissue Res. 2021;383:367–86.
36. Del Punta K, Leinders-Zufall T, Rodriguez I, Jukam D, Wysocki CJ, Ogawa S, et al. Deficient pheromone responses in mice lacking a cluster of vomeronasal receptor genes. Nature. 2002;419:70–4.
37. Jiang Y, Gong NN, Hu XS, Ni MJ, Pasi R, Matsunami H. Molecular profiling of activated olfactory neurons identifies odorant receptors for odors in vivo. Nat Neurosci. 2015;18:1446–54.
38. Silvotti L, Cavaliere RM, Belletti S, Tirindelli R. In-vivo activation of vomeronasal neurons shows adaptive responses to pheromonal stimuli. Sci Rep. 2018;8:8490.
39. Chamero P, Marton TF, Logan DW, Flanagan K, Cruz JR, Saghatelian A, et al. Identification of protein pheromones that promote aggressive behaviour. Nature. 2007;450:899–902.
40. Sturm T, Leinders-Zufall T, Maček B, Walzer M, Jung S, Pömmerl B, et al. Mouse urinary peptides provide a molecular basis for genotype discrimination by nasal sensory neurons. Nat Commun. 2013;4:1616.
41. Wong WM, Cao J, Zhang X, Doyle WI, Mercado LL, Gautron L, et al. Physiology-forward identification of bile acid-sensitive vomeronasal receptors. Sci Adv. 2020;6:eaaz6868.
42. Arakawa H, Cruz S, Deak T. From models to mechanisms: odorant communication as a key determinant of social behavior in rodents during illness-associated states. Neurosci Biobehav Rev. 2011;35:1916–28.
43. Liu H, Kai L, Du H, Wang X, Wang Y. LPS inhibits fatty acid absorption in enterocytes through TNF-alpha secreted by macrophages. Cells. 2019;8:1626.
44. Hu H, Cui Y, Yang Y. Circuits and functions of the lateral habenula in health and in disease. Nat Rev Neurosci. 2020;21:277–95.
45. Kwon J-T, Ryu C, Lee H, Sheffield A, Fan J, Cho DH, et al. An amygdala circuit that suppresses social engagement. Nature. 2021;593:114–8.
46. Kavaliers M, Choleris E. The role of social cognition in parasite and pathogen avoidance. Philos Trans R Soc Lond B Biol Sci. 2018;373(1751):20170206.
47. Kavaliers M, Ossenkopp KP, Choleris E. Pathogens, odors, and disgust in rodents. Neurosci Biobehav Rev. 2020;119:281–93.
48. Gervasi SS, Opiekun M, Martin T, Beauchamp GK, Kimball BA. Sharing an environment with sick conspecifics alters odors of healthy animals. Sci Rep. 2018;8:14255.
49. Hao L, Shi Y, Thomas S, Vezina CM, Bajpai S, Ashok A, et al. Comprehensive urinary metabolomic characterization of a genetically induced mouse model of prostatic inflammation. Int J Mass Spectrom. 2018;434:185–92.
50. Stacy A, Andrade-Oliveira V, McCulloch JA, Hild B, Oh JH, Perez-Chaparro PJ, et al. Infection trains the host for microbiota-enhanced resistance to pathogens. Cell. 2021;184:615-27 e17.
51. Uribe JH, Collado-Romero M, Zaldivar-Lopez S, Arce C, Bautista R, Carvajal A, et al. Transcriptional analysis of porcine intestinal mucosa infected with Salmonella Typhimurium revealed a massive inflammatory response and disruption of bile acid absorption in ileum. Vet Res. 2016;47:11.
52. Davis M. The role of the amygdala in conditioned and unconditioned fear and anxiety. In: Aggleton. JP, editor. The Amygdala. Oxford: Oxford University Press; 2000. 213–88.
53. Motta SC, Carobrez AP, Canteras NS. The periaqueductal gray and primal emotional processing critical to influence complex defensive responses, fear learning and reward seeking. Neurosci Biobehav Rev. 2017;76:39–47.
54. Canteras NS. The medial hypothalamic defensive system: hodological organization and functional implications. Pharmacol Biochem Behav. 2002;71:481–91.
55. Silva BA, Mattucci C, Krzywkowski P, Murana E, Illarionova A, Grinevich V, et al. Independent hypothalamic circuits for social and predator fear. Nat Neurosci. 2013;16:1731–3.
56. Mondoloni S, Mameli M, Congiu M. Reward and aversion encoding in the lateral habenula for innate and learned behaviours. Transl Psychiatry. 2022;12:3.
57. Sosa R, Mata-Luévanos J, Buenrostro-Jáuregui M. The role of the lateral habenula in inhibitory learning from reward omission. eNeuro. 2021;8(3):ENEURO.0016-21.2021.
58. Friard O, Gamba M. BORIS: a free, versatile open-source event-logging software for video/audio coding and live observations. Methods Ecol Evol. 2016;7:1325–30.
59. Bankhead P, Loughrey MB, Fernández JA, Dombrowski Y, McArt DG, Dunne PD, et al. QuPath: Open source software for digital pathology image analysis. Sci Rep. 2017;7:16878.
60. Schindelin J, Arganda-Carreras I, Frise E, Kaynig V, Longair M, Pietzsch T, et al. Fiji: an open-source platform for biological-image analysis. Nat Methods. 2012;9:676–82.

Publisher's Note